

AUTOMATIC REMOVAL OF SPARSE ARTIFACTS IN ELECTROENCEPHALOGRAM

Petr Tichavský, Miroslav Zima

*Institute of Information Theory and Automation, Pod vodárenskou věží 4, Prague, Czech Republic
Faculty of Nuclear Science and Physical Engineering, Czech Technical University in Prague, Prague, Czech Republic*

Vladimír Krajča

*Faculty Hospital Na Bulovce, Budínova 2, 182 00 Praha 8, Czech Republic
Czech Technical University in Prague, Faculty of Biomedical Engineering, Prague, Czech Republic*

Keywords: Artifact removal, Electroencephalogram, Independent component analysis, Second-order blind identification.

Abstract: In this paper we propose a method to identify and remove artifacts, that have a relatively short duration, from complex EEG data. The method is based on the application of an ICA algorithm to three non-overlapping partitions of a given data, selection of sparse independent components, removal of the component, and the combination of three resultant signal reconstructions in one final reconstruction. The method can be further enhanced by applying wavelet de-noising of the separated artifact components.

1 INTRODUCTION

Methods of the Independent Component Analysis (ICA) have been shown to be very useful in analyzing biomedical signals, such as EEG and MEG, see e.g. Makeig et al, 1996, Vigario, 2000, Joyce and Gorodnitsky, 2004, or James, 2005. In particular, it appears that these methods have an ability to separate unwanted parasitic signals (artifact), that have a relatively simple structure, from the useful biological signals, which are rich in information.

ICA/BSS methods usually use either non-Gaussianity, nonstationarity, a spectral diversity, or a combination of the three. In our paper, the artifact independent components are, by definition, sparse, and in the statistical sense this means that they are both nonstationary and non-Gaussian. Sometimes the artifact components also have a typical signature in the spectral domain. Therefore, any of the principles can be used to separate the sparse sources (artifacts), but not all methods have the same performance.

In the EEG signal processing, the most widely studied ICA algorithms are Infomax of Makeig et al (1996), SOBI of Belouchrani et al (1997), and FastICA of Hyvärinen and Oja (1997). While SOBI is based on the second-order statistics, the other two algorithms use high-order statistics. SOBI was advo-

cated by Romero (2008). In this paper, we mostly use an algorithm BGSEP, proposed by Pham and Cardoso (2001) implemented according to the paper of Tichavsky and Yeredor, 2009. BGSEP is based on second-order statistics as SOBI is, but it uses the non-stationarity of separated signals. While SOBI is done by approximate joint diagonalization (AJD) of a set of time-lagged covariance matrices of the signal (the mixture), BGSEP performs an AJD of zero lag covariance matrices in a partition of the signal.

In the context of the artifact removal it is desirable to have unwanted signals concentrated in a few separated components. The original data can be reconstructed without the artifact components using the estimated mixing matrix.

The artifact that we want to identify and separate have one common feature known as the *sparsity* in the time domain. This topic is elaborated on in Section II. The *sparse* artifacts include eye blinking and other ocular artifacts, various movement artifacts and unstuck electrode artifacts. The strong part of the proposed method consists of a robust combination of partial reconstructions obtained by processing mutually overlapping epochs of the EEG recording. Like the method of Castellanos and Makarov (2006), the proposed method aims to obtain a high quality of artifact removal at a negligible distortion of the cerebral EEG.

2 ARTIFACT REMOVAL IN ONE EPOCH

For the purpose of designing and testing artifact removal algorithms, we have considered three models of artifacts that are shown in Figure 1. These artifacts are inserted in an artifact-free EEG data at random times and in randomly chosen channels as shown in Figure 2. The models represent an eye blink, a body movement, and an unstuck electrode.

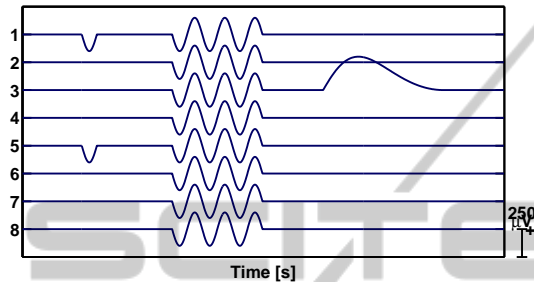


Figure 1: Models of artifacts.

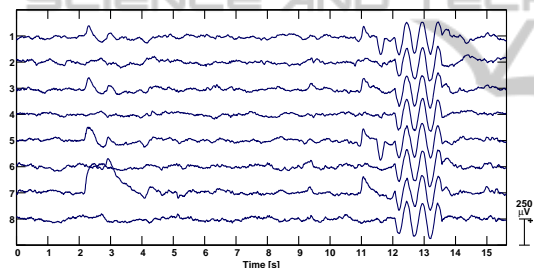


Figure 2: Example of neonatal EEG data with three embedded artifacts.

All artifacts under the consideration have one feature in common: their duration is short compared to the chosen epoch length. Such artifacts or signal components will be called *sparse* in the time domain. Usually, in the so called *compressive sensing*, the sparsity is measured as the count of the time instants in which the signal magnitude (absolute value) exceeds certain threshold. However, there is a problem in how large this threshold should be.

In this paper, we propose a simple ad hoc definition of the sparsity, which appears to perform well in our application. It is

$$\text{sparsity}(s^{(j)}) = \frac{\max[|s_i^{(j)}|]}{\text{std}[s_i^{(j)}]} \log \left(\frac{\text{std}[s_i^{(j)}]}{\text{median}[|s_i^{(j)}|]} \right) \quad (1)$$

where $s^{(j)} = (s_1^{(j)}, \dots, s_N^{(j)})$ is the j -th independent component, “std” stands for a standard deviation, and i is the time index, and N is the number of samples in the epoch. Note that the independent components are

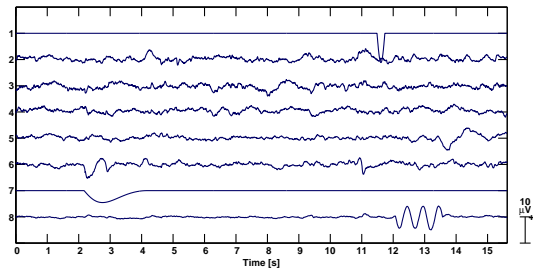


Figure 3: Independent component obtained by BGSEP for data in Figure 2. Sparsity (1) of the components is 115.2, 2.1, 1.4, 0.9, 3.2, 3.9, 42.0, and 7.7, respectively.

usually normalized to have the variance equal to one, so that $\text{std}[s_i^{(j)}] = 1$. The definition is motivated by the fact that the sparse components have large maximum absolute value, and simultaneously the median of the absolute value should be close to zero. We note, however, that the choice of the criterion of the sparsity is not crucial for our method, and our criterion can be easily replaced by another user-chosen criterion and a corresponding sparsity threshold.

For any definition of the sparsity, the component is regarded to be sparse (artifact), if its sparsity exceeds some threshold. The threshold is a design variable of the proposed artifact removal procedure. A higher value of the limit means a more conservative (a weaker) artifact reduction.

For example, independent components obtained by applying the algorithm BGSEP, and their sparsities (1) are shown in Figure 3. Note that the components 1, 6 and 7 have the largest sparsity and represent the separated artifacts. The figure suggests that the sparsity threshold should be set about five.






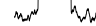


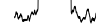
Since each artifact occupies one independent component, the number of artifacts in one epoch is upper bounded by the number of channels¹. Therefore, the proposed method cannot remove many artifacts in one time window, but only a few.

Among the independent components produced by an ICA algorithm, those with a sparsity exceeding a threshold are considered an artifact. In the reconstruction step, these components are replaced by zeros, and the reconstructed signal is computed by multiplying the matrix of the components by the estimated mixing matrix.

A detailed comparative study of the most popular ICA/BSS methods in terms of their ability to separate artifacts in EEG data was published in Delorme, 2007. Our simulations, not included here for lack of space show that the algorithm BGSEP also performs very well. Moreover, this method is very cheap com-

¹It is admitted that one artifact may affect several channels, but it must have the same shape in all channels.

Table 1: Three cases that may occur in combining three partial reconstructions in one (plus their permutations), where $\rho_{ij} = \|\mathbf{r}_i - \mathbf{r}_j\|^2$, $\mu_i = \max |\mathbf{r}_i|$, $i, j = 1, 2, 3$, $\rho_{\max} = \max\{\rho_{ij}\}$, $\rho_{\min} = \min\{\rho_{ij}\}$, $\mu_{\min} = \min\{\mu_i\}$.

	case A	case B	case C
\mathbf{r}_1			
\mathbf{r}_2			
\mathbf{r}_3			
$\rho_{\max} \leq 2\rho_{\min}$ or $\rho_{\max} \leq 2\rho_r$		$\mu_3 > \mu_{\min}$	$\mu_1 = \mu_{\min}$
$\mathbf{f} = \frac{\mathbf{r}_1 + \mathbf{r}_2 + \mathbf{r}_3}{3}$		$\rho_{12} = \rho_{\min}$	$\rho_{23} = \rho_{\min}$
		$\mathbf{f} = \frac{\mathbf{r}_1 + \mathbf{r}_2}{2}$	$\mathbf{f} = \mathbf{r}_1$

putationally.

Note that the artifact removal can be enhanced by wavelet de-noising of the to-be removed artifact components see Castellanos and Makarov, 2006. It has the positive effect of less removal of cerebral activity from the data.

3 ARTIFACT REMOVAL IN MULTIPLE EPOCHS

The data records that are encountered in EEG data processing are usually long. If the artifact removal is performed simply epoch by epoch, the performance may not always be satisfactory. Some artifacts can fall into two adjacent epochs and are masked. To increase robustness of the procedure, we found useful to perform the artifact removal in multiple epochs three times, each time with a different partitioning of the data into epochs.

The first partitioning of the time is $[1, N]$, $[N + 1, 2N]$, \dots , $[(n - 1)N + 1, nN]$, where N is the length of the epochs and n is the number of the epochs. n can be arbitrary. In the newborn EEG data, N is 1000-3000 samples, that is 10-20 seconds at 128 Hz or 256 Hz sampling.

The second partitioning of the time is $[1, N/3]$, $[N/3 + 1, 4N/3]$, \dots , $[N/3 + (n - 2)N + 1, nN - 2N/3]$, $[nN - 2N/3 + 1, nN]$. The artifact removal is performed only in the middle $n - 1$ epochs of the length N . In the first and in the last intervals, no artifact removal is performed.

The third partitioning is $[1, 2N/3]$, $[2N/3 + 1, 5N/3]$, \dots , $[nN - 4N/3 + 1, nN - N/3]$, $[nN - N/3 + 1, nN]$. Again, the artifact removal is performed only in the middle $n - 1$ epochs of the length N .

Each partitioning gives rise to one possible artifact-free reconstruction of the whole data. These

reconstructions are combined together in a special way so that the resulting reconstruction is generally smoother and more artifact-free than the partial reconstructions. An example of the three partitioning and corresponding reconstructions together with a final reconstruction is shown in Figure 5.

Combination of the three reconstructions into one proceeds sequentially, channel by channel, in time segments that are generally shorter than the epochs with the application of the ICA. They may have the form $[(k - 1)T_s + 1, kT_s]$, where T_s is the length of the segment (typically 200-300 samples).

Let \mathbf{r}_1 , \mathbf{r}_2 and \mathbf{r}_3 denote the three partial reconstructions in a channel in some (say the k -th) time segment. Let $\rho_{ij} = \|\mathbf{r}_i - \mathbf{r}_j\|^2$ denote the squared Euclidean distances of the reconstructions, $i, j = 1, 2, 3$, and let μ_i denote the maximum absolute value of elements of \mathbf{r}_i , $i = 1, 2, 3$. Let ρ_r denote the average squared norm $\|\mathbf{r}\|^2$ of a data segment \mathbf{r} of the same length as \mathbf{r}_i , randomly or systematically chosen in the whole available data, and let \mathbf{f} denote the desired final reconstruction. The choice of \mathbf{f} is summarized in Table 1.

In short, some of the three reconstructions might not be artifact-free and potentially still contain significant residua of the artifact. This possibility is presumably characterized by a relatively large μ_i . Therefore the proposed algorithm combines only "good" partial reconstructions. Depending on values of ρ_{ij} and μ_i , $i, j = 1, 2, 3$, \mathbf{f} is obtained as the average of one, two, or all three reconstructions.

4 SIMULATIONS

4.1 Removal of Artificial EEG Artifacts

In this subsection, performance of the proposed algorithm is studied on a visually noise-free EEG data set with five embedded artifacts, see figure 4a and 4b.

The proposed artifact removal procedure was applied with ICA (BGSEP with parameter 10) was computed in epochs of the length of 2500 samples (≈ 20 s). The time window for the reconstruction had 256 samples (2s). The limit sparsity was set to 3. Each artifact components was de-noised using the Matlab wavelet toolbox, the command `wden(data, 'minimaxi', 's', 'one', 7, 'sym5')`, prior its removal in each epoch and prior the synthesis of the three reconstructions. The resultant cleaned data and the estimated artifact (the noisy data minus the reconstruction) are shown in Figures 4(b) and 4(c), respectively. We note that the artifact removal is somewhat conservative, i.e. that the estimated

artifacts have a bit lower magnitude then the original (this is good).

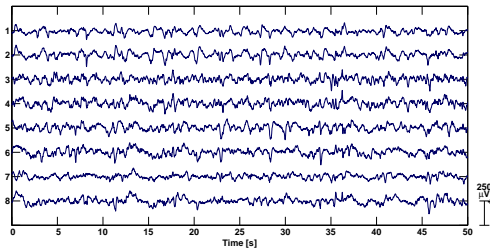


Figure 4(a): Original neonatal EEG data (a sleep).

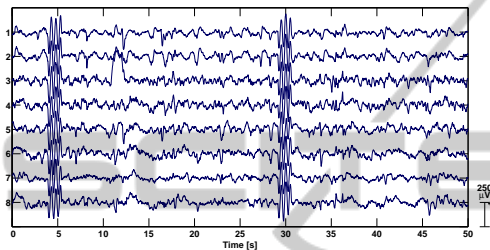


Figure 4(b): The same EEG data with a few inserted artifacts.

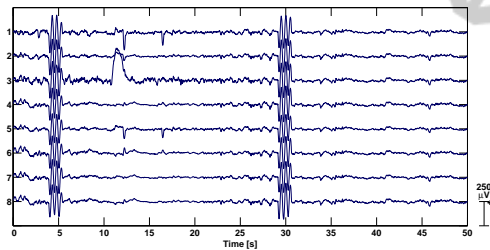


Figure 4(c): Estimated artifacts (without WD).

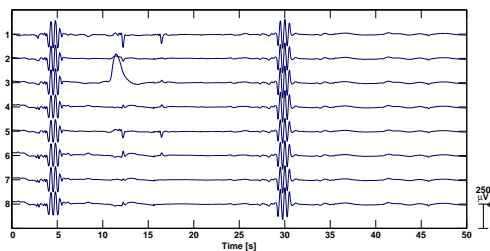


Figure 4(d): Estimated artifacts (with WD).

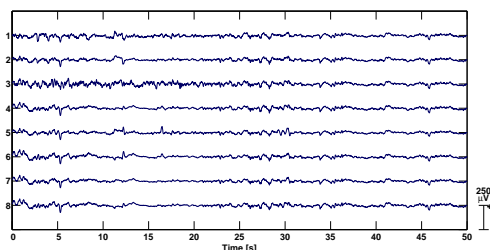


Figure 4(e): Error of the reconstruction (without WD).

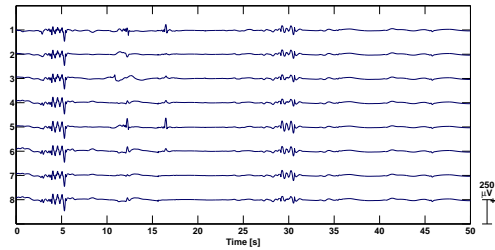


Figure 4(f): Error of the reconstruction (with WD).

We note that the error of the reconstruction, where the wavelet denoising of the artifact was applied, was greater than if it was absent.

4.2 Removal of Real EEG Artifacts

In this subsection, an example of performance of the proposed algorithm for the removal of real artifacts from EEG data is presented, see Figure 5(a). The main difference is that the ground truth (artifact-free signal) is not known. The EEG recording was sampled by 128 Hz. The epochs for ICA analysis had 2500 samples (≈ 20 s), and the time window for the reconstruction had 256 samples (2s). The results are shown in Figure 5(b)-(e). The three partial reconstructions and a final reconstruction of the component is shown in Figure 6. We note that not in all partial reconstructions the artifacts were sufficiently well suppressed, but the final reconstruction looks good.

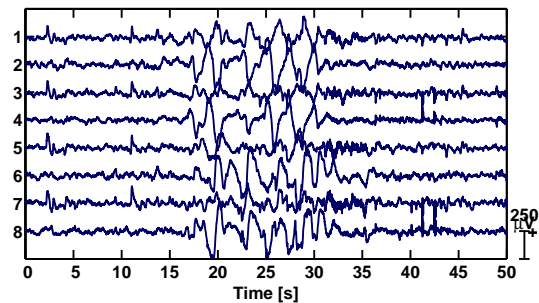


Figure 5(a): Neonatal EEG data with real movement artifact and eye blinking.

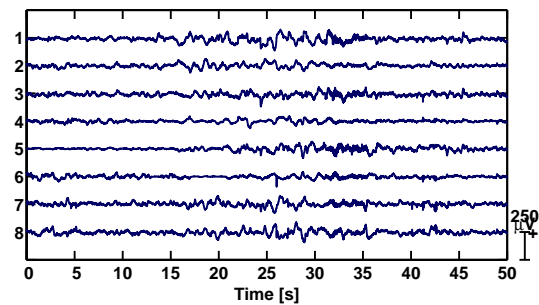


Figure 5(b): Removal of artifacts without WD.

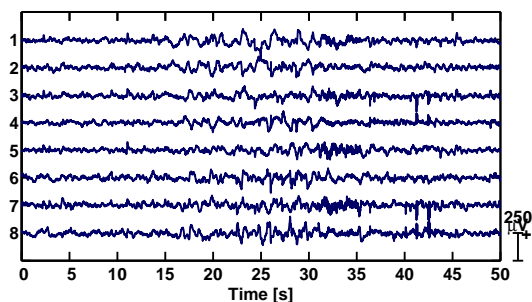


Figure 5(c): Removal of artifacts with WD.

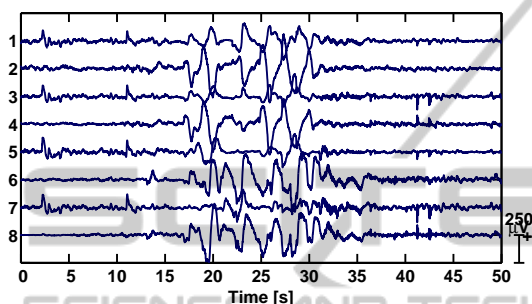


Figure 5(d): Estimated artifact (without WD).

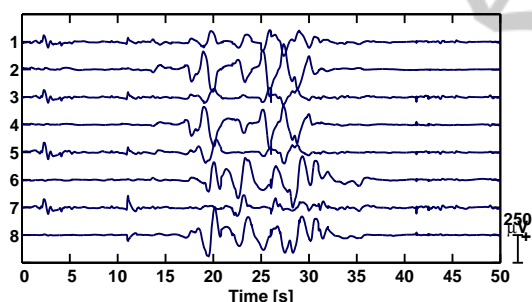


Figure 5(e): Estimated artifact (with WD).

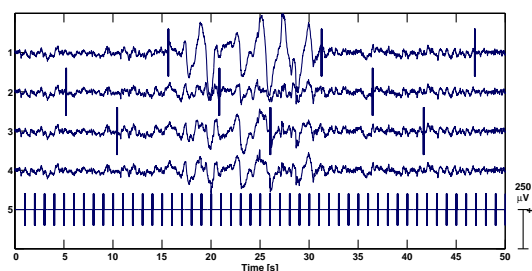


Figure 6: Three partial reconstructions of the 2nd channel in Figure 5 (epochs for the single frame artifact removal are marked by vertical lines), the final reconstruction, and intervals used for combining the partial reconstructions in one.

Note that the current implementation of the artifact separation procedure, which exists either in Matlab or in C++, allows processing a 10 minutes long 8

channel recording sampled at 256 Hz in about 10s on an ordinary PC with a 3GHz processor.

5 CONCLUSIONS

The presented method of artifact removal from data of arbitrary length is suitable for artifacts that have relatively short duration and exceed in the magnitude of the neighborhood signal. Examples include eye blinks or occasional body movement artifacts. The method is also fast in comparison with other ICA-based methods, because it uses a computationally effective method BGSEP. Increased robustness of the procedure is obtained by a sophisticated way of combining three ICA reconstructions. The method can be used, for example, as a data preprocessing for the identification of sleep stages of neonatal babies, but it is not limited to this kind of data. More details can be found in Zima et.al. (2010).

ACKNOWLEDGEMENTS

This work was supported by Ministry of Education, Youth and Sports of the Czech Republic through the project 1M0572 and by Grant Agency of the Czech Republic through the project 102/09/1278.

REFERENCES

- Belouchrani A, Abed-Meraim K, Cardoso J.F., Moulines E. (1997) A blind source separation technique using second-order statistics. *IEEE Transactions on Signal Processing* 1997; 45:434-444.
- Castellanos NP, Makarov V.A. (2006) Recovering EEG brain signals: Artifact suppression and wavelet enhanced independent component analysis. *J. Neuroscience Methods* 2006; 158:300-312.
- Delorme A, Sejnowski T., Makeig S. (2007) Enhanced detection of artifacts in EEG data using higher-order statistics and independent component analysis. *Neuroimage* 2007; 34:1443-1449.
- Hyvärinen A., Oja E. (1997) A fast fixed-point algorithm for independent component analysis. *Neural Computation* 1997; 9:1483-1492.
- James C.J., Hesse C.W. (2005) Independent component analysis for biomedical signals. *Physiological Measurements* 2005; 26:R15-R39.
- Joyce C.A., Gorodnitsky I.F., Kutas M. (2004), Automatic removal of eye movement and blink artifacts from EEG data using blind component separation. *Psychophysiology* 2004; 41:313-325.
- Makeig S., Bell A.J., Jung T.P., Sejnowski T.J. (1996) Independent component analysis of encephalographic data. *Adv. Neural Inf. Process. Syst.* 1996; 8:145-151.

- Pham D.T., Cardoso J.F. (2001). Blind separation of instantaneous mixtures of nonstationary sources. *IEEE Transactions on Signal Processing* 2001; 49:1837-1848.
- Romero S., Mananas M., Barbanoj M. (2008), A comparative study of automatic techniques for ocular artifact reduction in spontaneous EEG signals based on clinical target variables: A simulation case. *Computers in Biology and Medicine* 2008; 38:348-360.
- Tichavský P., Yeredor A. (2009) Fast approximate joint diagonalization incorporating weight matrices. *IEEE Transactions on Signal Processing* 2009; 57:878-891.
- Vigario R. (2000) Independent component approach to the analysis of EEG and MEG recordings. *IEEE Transactions on Biomedical Engineering* 2000; 47:589-593.
- Zima M., Tichavský P., and Krajča V. (2010) Automatic removal of sparse artifacts in electroencephalogram, Institute of Information Theory and Automation, Prague, Czech Republic, Technical Report No. 2289, November.

